



Compositional stratigraphy of clay-bearing layered deposits at Mawrth Vallis, Mars

J. J. Wray,¹ B. L. Ehlmann,² S. W. Squyres,¹ J. F. Mustard,² and R. L. Kirk³

Received 22 April 2008; revised 15 May 2008; accepted 19 May 2008; published 21 June 2008.

[1] Phyllosilicates have previously been detected in layered outcrops in and around the Martian outflow channel Mawrth Vallis. CRISM spectra of these outcrops exhibit features diagnostic of kaolinite, montmorillonite, and Fe/Mg-rich smectites, along with crystalline ferric oxide minerals such as hematite. These minerals occur in distinct stratigraphic horizons, implying changing environmental conditions and/or a variable sediment source for these layered deposits. Similar stratigraphic sequences occur on both sides of the outflow channel and on its floor, with Al-clay-bearing layers typically overlying Fe/Mg-clay-bearing layers. This pattern, combined with layer geometries measured using topographic data from HiRISE and HRSC, suggests that the Al-clay-bearing horizons at Mawrth Vallis postdate the outflow channel and may represent a later sedimentary or altered pyroclastic deposit that drapes the topography. **Citation:** Wray, J. J., B. L. Ehlmann, S. W. Squyres, J. F. Mustard, and R. L. Kirk (2008), Compositional stratigraphy of clay-bearing layered deposits at Mawrth Vallis, Mars, *Geophys. Res. Lett.*, 35, L12202, doi:10.1029/2008GL034385.

1. Introduction

[2] Phyllosilicate-bearing outcrops on Mars were first definitively identified by the OMEGA infrared spectrometer [Bibring *et al.*, 2005]. Subsequent studies have detected phyllosilicates in a variety of settings scattered across the planet, usually in materials of Noachian age [Poulet *et al.*, 2005; Bibring *et al.*, 2006; Mustard *et al.*, 2008]. Clay minerals may have formed at the surface in a neutral-to-alkaline aqueous environment, distinct from the more arid and acidic conditions inferred for much of the planet's subsequent history [e.g., Bibring *et al.*, 2006]. Alternatively, phyllosilicates may have formed in subsurface (e.g., hydrothermal) environments.

[3] OMEGA spectra have been used to identify two distinct phyllosilicate minerals in layered outcrops in and around Mawrth Vallis: Fe/Mg-rich smectite and the Al-rich smectite montmorillonite [Poulet *et al.*, 2005; Loizeau *et al.*, 2007]. Mawrth Vallis is an outflow channel that cuts Noachian cratered terrain in Western Arabia before debouching into the Chryse basin. Previous studies have interpreted the region's clay-bearing materials as ancient

sedimentary and/or altered pyroclastic deposits predating the Mawrth Vallis outflow(s) [Loizeau *et al.*, 2007; Michalski and Noe Dobrea, 2007]. Alternatively, Howard and Moore [2007] have suggested that these deposits may drape and thus postdate the outflow channel.

[4] In this study, we use Mars Reconnaissance Orbiter (MRO) data to refine the mineralogy and stratigraphy of the Mawrth Vallis layered materials. The stratigraphy at multiple sites, along with topographic data from HRSC and HiRISE, provides insight into the geometries of the clay-bearing layers at regional and outcrop scales, and constrains their age and mode of deposition.

2. Compositional Stratigraphy

[5] The spatial and spectral resolution of MRO instruments is well suited for studying compositional stratigraphy on Mars. At Mawrth Vallis, we use data from the CRISM infrared spectrometer [Murchie *et al.*, 2007] to identify geologic units of distinct composition, and then employ the 25–32 cm/pixel images of the HiRISE camera [McEwen *et al.*, 2007] to reveal stratigraphic relationships among units. Dozens of HiRISE images and CRISM targeted observations (~18 or 36 m/pixel) of the ~300 × 400 km region around Mawrth Vallis exist as of this writing; we focus on coordinated HiRISE-CRISM observations (Figure 1).

[6] Simple atmospheric and photometric corrections are applied to CRISM data [Mustard *et al.*, 2008]. Spectral summary parameter band depth maps for absorptions at 1.9, 2.2, and 2.3 μm are used to map the spatial distribution of phyllosilicate-bearing minerals [Pelkey *et al.*, 2007]. The 1.9 μm absorption band results from H₂O in hydrated minerals. Combination tones of cation-OH stretches result in absorptions at 2.2 μm for Al-rich phyllosilicates and between 2.28–2.35 μm for Fe/Mg-rich phyllosilicates [Bishop *et al.*, 2002]. We compute spectral ratios between regions of interest (>50 pixels in size) and large regions of dust or material of low spectral contrast within the scene, to highlight compositional differences [Poulet *et al.*, 2005; Mustard *et al.*, 2008] and facilitate comparison with library mineral spectra [Murchie *et al.*, 2007; Clark *et al.*, 2007].

2.1. Compositional and Morphologic Diversity

[7] The southern wall of the Mawrth Vallis channel provides superb stratigraphic exposures. CRISM spectral parameter maps overlain on a HiRISE image (Figure 2a) show a clear stratigraphic sequence, with Mg/Fe-phyllosilicate-bearing layers (1) overlying Al-clay-bearing layers (2), which overlie another Fe/Mg-clay-bearing unit (4). Between stratigraphic units 2 and 4 is a layer exhibiting a hydration band, but comparatively weak metal-OH bands (3), possibly

¹Department of Astronomy, Cornell University, Ithaca, New York, USA.

²Department of Geological Sciences, Brown University, Providence, Rhode Island, USA.

³Astrogeology Program, U.S. Geological Survey, Flagstaff, Arizona, USA.

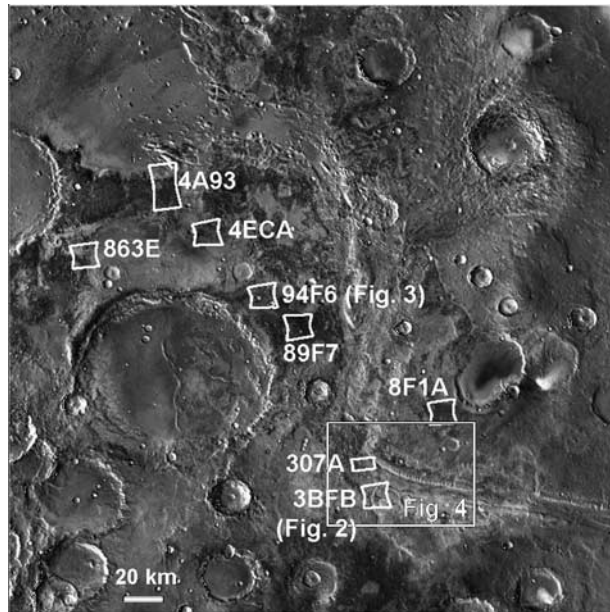


Figure 1. THEMIS IR mosaic of Mawrth Vallis region. CRISM footprints and image identifiers are shown for images mentioned in the text; 307A and 4A93 are half-resolution (~ 36 m/pixel), while others are full resolution.

a mixture of units 2 and 4. Corresponding CRISM ratio spectra (Figure 2b) show that unit 4 has a band centered at $2.29 \mu\text{m}$ and a strong $1.9 \mu\text{m}$ H_2O band, while unit 1 has a band centered at $2.31 \mu\text{m}$ and a negligible $1.9 \mu\text{m}$ H_2O band. Unit 4 contains an Fe/Mg-smectite clay such as ferrosaponite or Mg-nontronite while unit 1 is consistent with a more Mg-rich phyllosilicate with negligible inter-layer water. Unit 2 has bands at 1.9 and $2.2 \mu\text{m}$, diagnostic of hydrated Al-bearing phyllosilicates. The slight doublet at $2.2 \mu\text{m}$ indicates a kaolinite group mineral such as kaolinite or dickite associated with the hydrated Al-smectite montmorillonite. Bishop *et al.* [2008] have reported kaolinite at other locations around Mawrth Vallis. In addition to these H_2O and OH-related bands, the shape of CRISM ratio spectra shortward of $1 \mu\text{m}$ is consistent with the presence of hematite or other crystalline ferric oxide minerals [e.g., Morris *et al.*, 2000]. Variation of an iron oxide component with an absorption between 0.8 and $0.9 \mu\text{m}$ is especially evident in unit 2 and suggests subunits of distinct ferric oxide + Al-phyllosilicate composition (e.g., units 2a/b in Figure 2b).

[8] Each of these compositional units has a distinctive morphology. Unit 1 (Figure 2c) has sparse bright-rimmed fractures; similar features elsewhere on Mars have been interpreted as zones of localized alteration by subsurface fluids [Okubo and McEwen, 2007]. Units 2 and 3 (Figures 2d and 2e) are fractured into polygons ranging in diameter from under a meter (unit 2) to 5–10 meters (unit 3). As noted by Loizeau *et al.* [2007], polygons may have formed through desiccation and/or thermal contraction. Unit 4 (Figure 2f) is densely fractured and has quasi-circular albedo features that may be degraded remnants of impact craters. Each unit also has a distinct color in HiRISE images, as observed elsewhere in the Mawrth Vallis region (e.g., Figure 3). In general, units with Al-clays appear bluer

(blue to white depending on iron oxide content) than units with Fe/Mg-phyllosilicates. Loizeau *et al.* [2008] report a similar correlation between HRSC image color and phyllosilicate mineralogy derived from OMEGA.

[9] Elsewhere, impact craters provide excellent stratigraphic exposures. In one example west of the outflow channel, a ~ 4 -km crater exposes six units of distinct composition (Figure 3). Each phyllosilicate-ferric oxide mineral assemblage is confined to certain layers in the crater wall. CRISM ratio spectra (Figure 3b) of the Al-clay-bearing units here are consistent with the presence of kaolinite with varying hematite content. Fe/Mg-smectite-bearing units underlie the kaolinite-ferric oxide unit. Some Fe/Mg-smectite-bearing layers appear deformed, while adjacent layers appear undeformed (Figure 3d). The folded layers may have undergone syndepositional (e.g., soft sediment) deformation or may have resulted from strain partitioning within weaker multilayers, e.g. where the bedding is thinner. Alternatively, cross-beds deposited on a complex surface may explain the observed geometries. All clay-bearing units here and throughout the region are unconformably overlain by a darker, heavily cratered mantle deposit [Michalski and Noe Dobrea, 2007]; Loizeau *et al.* [2007] report pyroxene in this mantle, while clay minerals are not observed.

2.2. Similarity of Layer Sequences

[10] Beyond the two locations described above, we have examined four coordinated HiRISE-CRISM observations west of the outflow channel (CRISM HRL 4A93 and FRTs 89F7, 4ECA, and 863E), one northeast of the channel (FRT 8F1A), and one on the channel floor (HRS 307A). Both Al-clays and Fe/Mg-phyllosilicates are observed in every scene, and the Al-clays typically overlie the Fe/Mg-clays. An intervening hydrated unit analogous to unit 3 in Figure 2 is seen in some cases, but not all. An inverted stratigraphy is occasionally seen in impact crater ejecta. The only other exception we have found is at the location shown in Figure 2, where the Mg/Fe-phyllosilicate-bearing unit 1 overlies the Al-clay-bearing unit 2; however, the composition of unit 1 is not that of typical Fe/Mg-smectite clay and it may result from a different process. No observations to date show multiple Al-clay-bearing units separated stratigraphically by Fe/Mg-clay-bearing materials. Therefore, many of the Al-clay exposures in this region may be stratigraphically correlated in a single unit, a hypothesis that can be tested with topographic data.

3. Topography

3.1. Regional Geometry of Compositional Units

[11] To probe the regional geometry of the clay-bearing layers, we use a digital elevation model (DEM) derived from an HRSC image [Neukum and Jaumann, 2004] as outlined by Dumke *et al.* [2008]. The HRSC observation h1293_0000 (Figure 4a) covers most of the Mawrth Vallis channel at ~ 50 m/pixel in the color bands.

[12] Our DEM derived from this image has 50 m grid spacing. We measure strike and dip angles of contacts between units of different color in the HRSC color composite, using multi-linear regression to find the best-fit plane through a set of points. At least six points along a contact are used for each measurement shown here. All measured

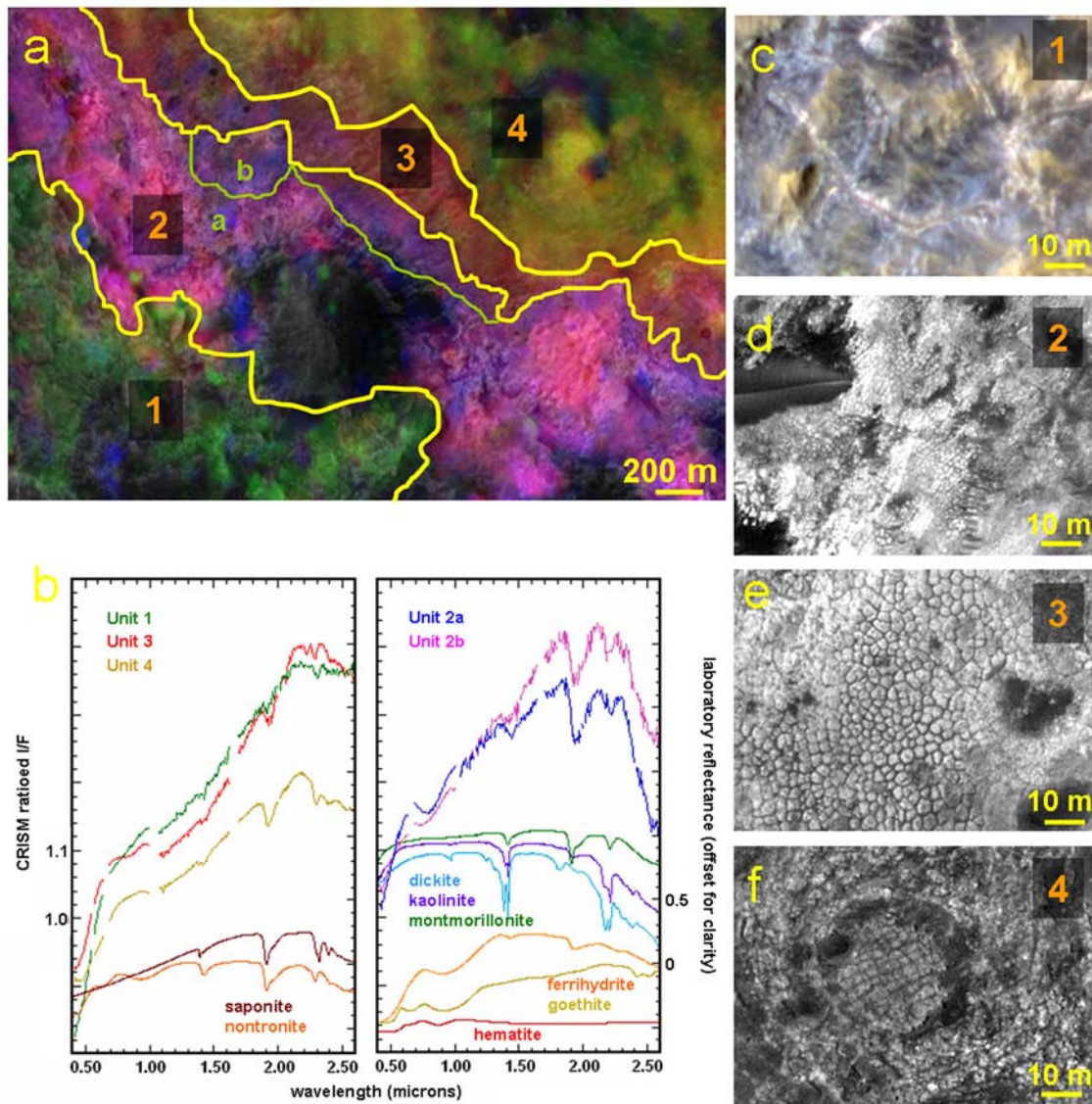


Figure 2. (a) Maps of band depth at $1.9 \mu\text{m}$ (red), $2.3 \mu\text{m}$ (green), and $2.2 \mu\text{m}$ (blue) indicative of hydration, Fe/Mg-phyllsilicates, and Al-phyllsilicates, respectively. Band maps from a portion of CRISM FRT 3BFB overlay on HiRISE PSP_002140_2025. Area slopes down toward upper right. (b) CRISM ratio spectra of compositional units in Figure 2a compared to library spectra. Units 2a and 2b are subunits within unit 2 with distinct spectral shapes shortward of $1 \mu\text{m}$, indicating ferric oxide variation. Morphology of (c) unit 1, showing bright-rimmed fractures; (d) unit 2, with meter-scale polygonal fractures; (e) unit 3, which has larger polygons; and (f) unit 4.

contacts are between relatively blue or white layers and underlying redder layers, interpreted to correspond to occurrences of Al-clays and Fe/Mg-phyllsilicates, respectively [Loizeau *et al.*, 2008]. These contacts may be equivalent to those between units 2/3 or 3/4 in Figure 2, or 2/4 in cases where unit 3 is not observed; we cannot clearly distinguish the relatively thin unit 3 with HRSC data alone.

[13] As Figure 4 shows, the contacts exposed in both channel walls dip toward the channel floor, with typical dip angles $\sim 3^\circ$. Dips range from 1.0° to 4.2° , with typical uncertainties of $\sim 1.0^\circ$ (95% confidence level). These dips are consistent with the average slopes of the unmantled upper channel walls (Figure 4b); the measured contacts are exposed on locally steeper slopes. Contacts on the channel

floor have measured dip angles $< 1^\circ$, dipping generally downstream.

[14] The eastern half of the channel segment shown in Figure 4a has a break in wall slope ~ 400 meters above the channel floor (Figure 4c), below which both walls are steeper ($\sim 10^\circ$). However, the lower walls are completely obscured by the dark mantle deposit, so we cannot determine whether the contacts dip more steeply here (as expected if they correlate with contacts on the channel floor), or instead are cut by the lower channel walls. Although we cannot exclude the possibility of repeating stratigraphic sequences that are cut by the channel, yet hidden beneath the dark mantle, such repeating sequences are not observed in CTX and HRSC images of the unmantled channel wall on the western side of Figure 4a. The

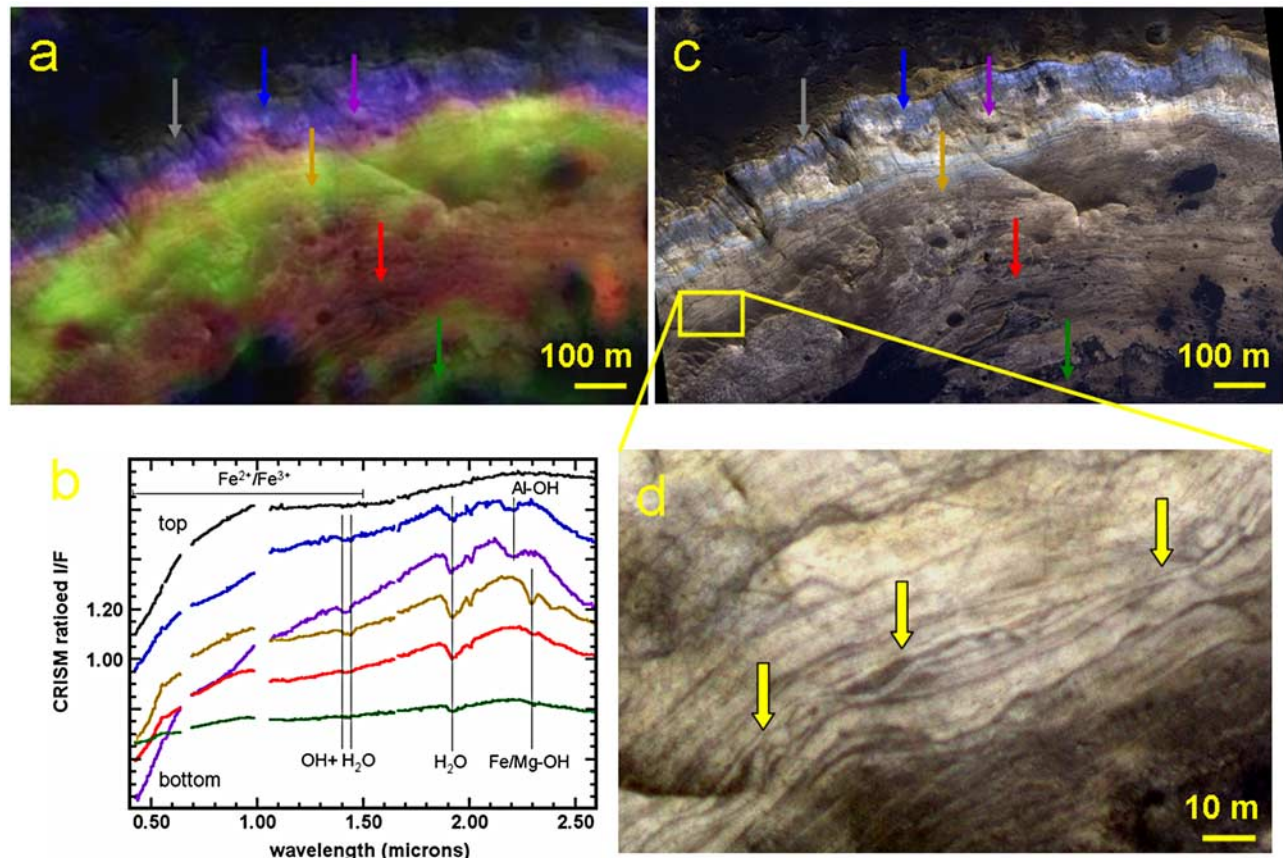


Figure 3. (a) Compositional stratigraphy exposed in the northern wall of a 4-km crater. CRISM FRT 94F6 band depth overlain on HiRISE PSP_004052_2045 with colors as in Figure 2. (b) CRISM ratio spectra of six distinct layers in Figure 3a; see text for discussion. (c) Color HiRISE image of the crater wall, with IR/Red/Blue-green bands (874/694/536 nm) mapped to R/G/B. (d) Some Fe/Mg-clay-bearing layers appear folded.

overall conformity of the exposed contacts to the topography of the channel walls and floor supports the hypothesis that the bluer, typically Al-clay-bearing outcrops occupy a single unit that drapes over the outflow channel.

[15] We have observed no contact between the redder, Fe/Mg-clay-bearing materials and any underlying units in MRO data. We thus cannot constrain the regional geometry of this unit, and its clays—and/or the layers containing them—may predate the outflow channel.

3.2. Geometry of Meter-Scale Layers

[16] We use a DEM derived from HiRISE images to verify our HRSC measurements and measure the geometries of individual layers of meter-to-decameter thickness. Layer geometries constrain modes of deposition; e.g., airfall layers should drape preexisting topography.

[17] Our HiRISE DEM has 1 m grid spacing, and is derived from images PSP_002074_2025 and PSP_002140_2025 via techniques described by R. L. Kirk et al. (Ultrahigh resolution topographic mapping of Mars with MRO HiRISE stereo images: Meter-scale slopes of candidate Phoenix landing sites, submitted to *Journal of Geophysical Research*, 2008). This DEM covers an area of $\sim 6 \times 20$ km on the southern channel wall (outlined in Figure 4a), including the area of Figure 2a.

[18] By fitting planes to the unit 1/2 and unit 2/3 contacts, we have measured the true thickness of the Al-clay-bearing

unit 2 at several points along the section shown in Figure 2a, yielding a mean value of 41 ± 14 m. The unit 2/3 contact has $3.2 \pm 0.6^\circ$ dip, $24.8 \pm 12.1^\circ$ dip direction (clockwise from North); the HRSC DEM measurement of the same contact yields a dip of $2.5 \pm 0.5^\circ$ and dip direction of $0.5 \pm 13.9^\circ$. Similarly, the unit 3/4 contact has $2.9 \pm 0.7^\circ$ dip and $12.9 \pm 14.1^\circ$ dip direction in the HiRISE DEM. Thus the unit contact geometries measured in the HiRISE DEM agree with HRSC DEM measurements.

[19] From 14 individual layers within unit 2 spread across the HiRISE DEM, we compute an average dip of 8.5° and an average dip direction of 40° , notably steeper and slightly more easterly than the unit 2/3 contact. Measured layer dips range from 3.6° to 15.6° , with typical uncertainties $\sim 2^\circ$ (95% confidence level); dip directions range from 334° to 99° , with typical uncertainties $\sim 17^\circ$. Unfortunately, the other units—including the Fe/Mg-clay-bearing materials—exhibit few well-defined layers within the DEM, so we cannot compare their orientations to those of the layers in unit 2.

4. Discussion

[20] Our conclusion—based on HRSC topography and high-resolution stratigraphy from HiRISE and CRISM—that the Al-rich clays at Mawrth Vallis may occupy a single unit (unit 2) that drapes the outflow channel differs from con-

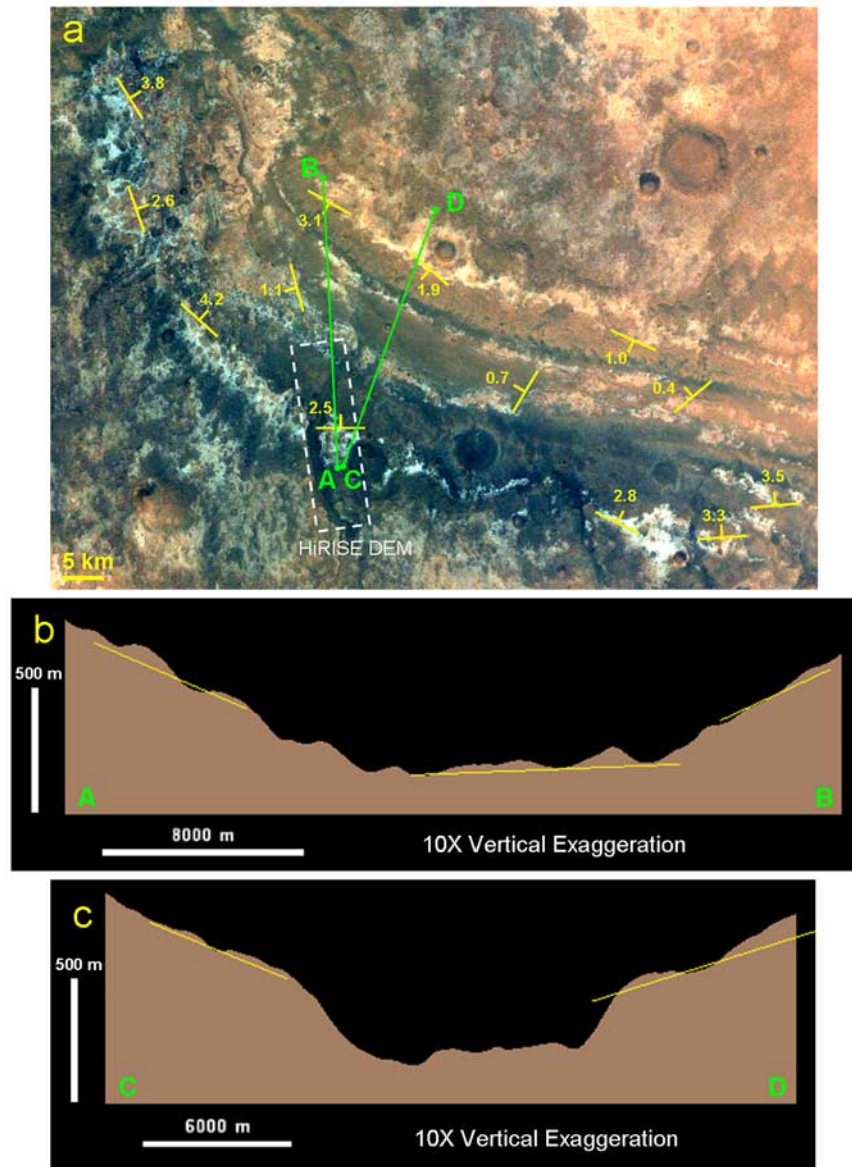


Figure 4. (a) A portion of the HRSC color image h1293_0000, showing southeast Mawrth Vallis. Strike and dip measurements (degrees) from the HRSC DEM are superposed. (b) HRSC elevation profile across channel walls and floor; measured contact orientations (yellow line segments) conform to channel topography. (c) Elevation profile displaying break in wall slope ~ 400 m above the channel floor, as discussed in the text.

clusions of prior studies [Poulet *et al.*, 2005; Loizeau *et al.*, 2007]. Howard and Moore [2007] reach a similar conclusion, but do not distinguish between units of different clay composition. Mawrth Vallis is the oldest of the circum-Chryse outflow channels, with a mid-to-late Noachian age estimated from crater counts [Ivanov and Head, 2001]. Thus, emplacement of these clays may still have occurred in the Noachian or early Hesperian, consistent with the presence of the heavily cratered mantle overlying the clay-bearing units. Furthermore, if the Al-clay unit is sedimentary, then the clay-forming alteration event(s) may have occurred even earlier at another location, with subsequent erosion and transport carrying the clays to Mawrth Vallis.

[21] An alternative hypothesis is that the Al-clay-bearing unit formed through *in situ* alteration—confined to the upper few decameters—of compositionally homogeneous

materials during the late Noachian. The contact between the Al-clay-bearing unit and Fe/Mg-clay-bearing unit would then represent an alteration front; Noe Dobrea *et al.* [2008] propose a similar hypothesis. Greater throughflow of water in the upper decameters could have leached Mg, Fe, and Ca cations, yielding a more Al-rich clay composition. However, Al-clay signatures are confined to particular layers in the stratigraphy, which have a distinctive morphology (Figure 2d), suggesting that they occupy a distinct lithologic unit that drapes the outflow channel. This unit may be either sedimentary or pyroclastic in origin. Volcanic glasses in a pyroclastic deposit could be relatively easily altered into clays. However, the fact that individual layers within this unit do not conform to the unit 2/3 contact as measured in our HiRISE DEM argues against airfall emplacement of these layers. If their origin is sedimentary, then

the subunits of distinct ferric oxide and Al-clay composition within unit 2 may reflect a changing sediment source.

[22] Regardless, the presence of diverse minerals in a clear stratigraphic sequence implies that the layered materials at Mawrth Vallis record a time series of environmental change. This fact, in addition to the role of water in forming the mineralogies and morphologies visible at the surface today, is perhaps the best argument for future exploration of Mawrth Vallis by surface missions seeking evidence for ancient habitable environments on Mars.

[23] **Acknowledgments.** We thank M. Rosiek and A. Dumke for their efforts producing HiRISE and HRSC DEMs, respectively. C. Okubo provided helpful suggestions on DEM analysis. Comments from A.S. McEwen, R.E. Milliken, N.T. Bridges, E.Z. Noe Dobrea, B.J. Thomson, F. Poulet, and our reviewers improved the paper. JJW thanks the Fannie & John Hertz Foundation for support.

References

- Bibring, J.-P., et al. (2005), Mars surface diversity as revealed by the OMEGA/Mars Express observations, *Science*, 307(5715), 1576–1581, doi:10.1126/science.1108806.
- Bibring, J.-P., et al. (2006), Global mineralogical and aqueous Mars history derived from OMEGA/Mars Express data, *Science*, 312(5772), 400–404, doi:10.1126/science.1122659.
- Bishop, J. L., E. Murad, and M. D. Dyar (2002), The influence of octahedral and tetrahedral cation substitution on the structure of smectites and serpentines as observed through infrared spectroscopy, *Clay Miner.*, 37(4), 617–628.
- Bishop, J. L., et al. (2008), Phyllosilicate diversity observed by CRISM in Mawrth Vallis: Identification of nontronite, montmorillonite, kaolinite, and hydrated silica, *Lunar Planet. Sci.*, XXXIX, Abstract 2124.
- Clark, R. N., et al. (2007), USGS digital spectral library splib06a, *Digital Data Ser. 231*, U. S. Geol. Surv., Denver, Colo. (Available at <http://speclab.cr.usgs.gov/spectral.lib06>)
- Dumke, A., M. Spiegel, R. Schmidt, and G. Neukum (2008), High-resolution digital terrain models and ortho-image mosaics of Mars: Generation on the basis of Mars-Express HRSC data, *Lunar Planet. Sci.*, XXXIX, Abstract 1910.
- Howard, A. D., and J. H. Moore (2007), The light-toned sediments in and near lower Mawrth Vallis may be a drape deposit, *Lunar Planet. Sci.*, XXXVIII, Abstract 1339.
- Ivanov, M. A., and J. W. Head (2001), Chryse Planitia, Mars: Topographic configuration, outflow channel continuity and sequence, and tests for hypothesized ancient bodies of water using Mars Orbiter Laser Altimeter (MOLA) data, *J. Geophys. Res.*, 106(E2), 3275–3296, doi:10.1029/2000JE001257.
- Loizeau, D., et al. (2007), Phyllosilicates in the Mawrth Vallis region of Mars, *J. Geophys. Res.*, 112, E08S08, doi:10.1029/2006JE002877.
- Loizeau, D., N. Mangold, F. Poulet, V. Ansan, E. Hauber, J.-P. Bibring, Y. Langevin, B. Gondet, P. Masson, and G. Neukum (2008), Stratigraphy of the Mawrth Vallis region through OMEGA, HRSC color imagery and DTM, *Lunar Planet. Sci.*, XXXIX, Abstract 1586.
- McEwen, A. S., et al. (2007), Mars Reconnaissance Orbiter's High Resolution Imaging Science Experiment (HiRISE), *J. Geophys. Res.*, 112, E05S02, doi:10.1029/2005JE002605.
- Michalski, J. R., and E. Z. Noe Dobrea (2007), Evidence for a sedimentary origin of clay minerals in the Mawrth Vallis region, Mars, *Geology*, 35(10), 951–954, doi:10.1130/G23854A.
- Morris, R. V., et al. (2000), Mineralogy, composition, and alteration of Mars Pathfinder rocks and soils: Evidence from multispectral, elemental, and magnetic data on terrestrial analogue, SNC meteorite, and Pathfinder samples, *J. Geophys. Res.*, 105(E1), 1757–1817, doi:10.1029/1999JE001059.
- Murchie, S., et al. (2007), Compact Reconnaissance Imaging Spectrometer for Mars (CRISM) on Mars Reconnaissance Orbiter (MRO), *J. Geophys. Res.*, 112, E05S03, doi:10.1029/2006JE002682.
- Mustard, J. F., et al. (2008), Hydrated silicate minerals on Mars observed by the Mars Reconnaissance Orbiter CRISM instrument, *Nature*, doi:10.1038/nature07097, in press.
- Neukum, G., and R. Jaumann (2004), HRSC: The High Resolution Stereo Camera of Mars Express, in *Mars Express: The Scientific Payload*, edited by A. Wilson, *Eur. Space Agency Spec. Publ., ESA-SP 1240*, 17–35.
- Noe Dobrea, E. Z., et al. (2008), Clay bearing units in the region around Mawrth Vallis: Stratigraphy, extent, and possible alteration fronts, *Lunar Planet. Sci.*, XXXIX, Abstract 1077.
- Okubo, C. H., and A. S. McEwen (2007), Fracture-controlled paleo-fluid flow in Candor Chasma, Mars, *Science*, 315(5814), 983–985, doi:10.1126/science.1136855.
- Pelkey, S. M., et al. (2007), CRISM multispectral summary products: Parameterizing mineral diversity on Mars from reflectance, *J. Geophys. Res.*, 112, E08S14, doi:10.1029/2006JE002831.
- Poulet, F., J.-P. Bibring, J. F. Mustard, A. Gendrin, N. Mangold, Y. Langevin, R. E. Arvidson, B. Gondet, C. Gomez, and The Omega Team (2005), Phyllosilicates on Mars and implications for early Martian climate, *Nature*, 438(7068), 623–627, doi:10.1038/nature04274.
- B. L. Ehlmann and J. F. Mustard, Department of Geological Sciences, Brown University, Providence, RI 02912, USA.
- R. L. Kirk, Astrogeology Program, U.S. Geological Survey, Flagstaff, AZ 86001, USA.
- S. W. Squyres and J. J. Wray, Department of Astronomy, Cornell University, Ithaca, NY 14853, USA. (jwray@astro.cornell.edu)